energies

MDPI

Article

Experimental Studies of Fluid Flow Resistance in a Heat Exchanger Based on the Triply Periodic Minimal Surface

Marcin Kruzel, Krzysztof Dutkowski * and Tadeusz Bohdal

Department of Mechanical and Power Engineering, Koszalin University of Technology, 78-453 Koszalin, Poland; marcin.kruzel@tu.koszalin.pl (M.K.); tadeusz.bohdal@tu.koszalin.pl (T.B.)
* Correspondence: krzysztof.dutkowski@tu.koszalin.pl

Abstract: This study describes experimental data on 3D-printed compact heat exchangers. The heat exchanger is a prototype designed and manufactured additively using 3D printing in metal—AISI 316L steel. The device's design is based on the triply periodic minimal surface (TPMS) geometry called gyroid, which can only be obtained by incremental manufacturing. This innovative heat exchange surface structure enables these devices to provide higher thermal performance while reducing their weight by up to 50%. Few publications describe thermal or flow tests in this type of device. They mainly concern computer simulations that have yet to be experimentally verified. The authors of this study conducted innovative flow tests to determine pressure drops during the flow of working fluids under conditions of variable temperature, mass flow rate and thermal load. Water was used as a heat transfer fluid during the tests. The range of parameters for the entire experiment was $\dot{m}$ = 1–24 kg/h; $\Delta p/\Delta l$ = 0.05–2 kPa; t_{cold} = 20 °C; t_{hot} = 50 °C. Flow characteristics during the single-phase heat exchange process were determined, including $\Delta p/\Delta l = f(\dot{m})$, $\Delta p/\Delta l = f(Re)$, $\Delta p/\Delta l = f(f)$. The experimental data will be used to determine the relationships describing flow resistance in structures based on a triply periodic minimal surface, and it also enables one to specify the energy consumption of these devices and compare the profitability of their use to conventional designs, i.e., shell-and-tube or plate heat exchangers.

Keywords: TPMS; gyroid; pressure drop; heat exchanger; friction factor

Academic Editor: Robert Kaniowski

Received: 26 November 2024
Revised: 18 December 2024
Accepted: 31 December 2024
Published: 1 January 2025

Citation: Kruzel, M.; Dutkowski, K.; Bohdal, T. Experimental Studies of Fluid Flow Resistance in a Heat Exchanger Based on the Triply Periodic Minimal Surface. *Energies* **2025**, *18*, 134. https://doi.org/10.3390/en18010134

1. Introduction

Modern heat exchanger designs are becoming more and more complex. Their complexity positively affects the thermal parameters of the heat transfer process. Unfortunately, as the thermal parameters increase, flow resistance is observed. This translates into the need to engage more driving energy of the working fluid pumps. Only a few works have been published describing flow resistance in heat exchangers based on TPMS geometries.

Reynolds et al. [1] described the results of testing flow heat exchangers based on TPMSs. The presented data proved that the TPMS design provided a high heat transfer rate and acceptable flow resistance. The TPMS lattice was further investigated to determine performance with variable porosity levels ranging up to 85%, hydraulic diameters from 2 to 10 mm, and wall thicknesses between 0.4 and 2.6 mm. Samson et al. [2] studied pressure drops in triply periodic minimal surfaces. The dependence of cell size and linear flow losses shows that smaller cell sizes exhibit a more significant specific pressure drop. Oh et al. [3] conducted pressure drop tests using appropriate heat exchangers based on TPMS structures made of polymer and found that the resulting pressure drop was reduced by 85%. Heat

transfer tests were also carried out using an optimal metal structure. The obtained heat transfer capacity (i.e., overall heat transfer coefficient) was significant compared to the case of typical solutions, proving that the developed functional gradations of TPMS structures increase the capacity heat exchange of heat exchangers manufactured using the additive method. Wang et al. [4] studied the flow and heat transfer in different channels based on triple periodic minimum surfaces (TPMSs). Flow resistance and HTC in Neovius channels were the most responsive to the cell volume fraction (R). The topology differences and heat transfer mechanisms determined that Neovius channels provided the best HTC values at $R < 0.5$, while F-KS channels had the best values when $R > 0.5$. Of the four topologies, the thermohydraulic performance of I-WP is the most sensitive to R, while the Primitive structure is the least sensitive.

Most of the presented studies concern numerical data. Bonner-Hutton et al. numerically studied pressure drop in compact heat exchangers [5]. The performance of each heat exchanger design was assessed based on the total heat transfer coefficient and pressure loss. The results confirmed the greater efficiency and effectiveness of the gyroid heat exchanger design, which was also confirmed based on additional analytical calculations. Tang et al. [6] analyzed the convective heat transfer process and triple periodic minimum surface (TPMS) performance based on Diamond, gyroid and Iwp (I-Graph-Wrapped Package) structures on spatially oriented unfolded surfaces. Pressure drops and heat transfer in the above range were also described by Tang et al. in [6], which analyzed the convective heat transfer process and the performance of triple periodic minimum surfaces (TPMSs) based on Diamond, gyroid and Iwp structures on spatially oriented unfolded surfaces. The study's authors also described pressure drops and heat transfer in the above range [7]. Numerical simulations showed that the optimization could improve the convective heat transfer efficiency of the gyroid and reduce the flow resistance. Studies [6,7] also presented heat transfer efficiency in Diamond, gyroid and Iwp TPMS structures. In [8], a heat exchanger was tested. Brambati et al. aimed to formulate an HTC based on numerical data. Dassi et al. [9] compared numerical and experimental data of the cooling circuit of journal bearings. Good data agreement was found. Chen et al. [10] conducted a numerical study on improving heat transfer in a gyroidal HX. Also, 3D-printed compact heat exchangers were tested by Dixit et al. [11]. The authors confirmed a 55% improvement in heat transfer in 3D-printed gyroid heat exchangers compared to a common heat exchanger. The thermophysical properties of a filament used for manufacturing heat exchanger additives were presented in [12–14]. Moradmand et al. [15] presented experimental and numerical data on the thermal efficiency of gyroid and Schwarz-P structure heat exchangers. Good data agreements were found. Yan et al. [16] numerically studied a TPMS HX. A significant increase in HTC value was found for the TPMS-based heat exchanger design. The study in [17] presents the thermo-hydraulic parameters of a gyroid HX. Liang et al. [18] numerically studied the effect of the size of the unit on the flow resistance and the HTC value in the Diamond HX. In [19], the thermal efficiency of a single cube manufactured using three TPMS structures was analyzed. The gyroid cube had the highest HTC. Alteneiji et al. [20] built patterns that address the proposed heat exchanger's heat transfer efficiency (ε) and number of transmission units. In [21], a copper TPMS HX was built and tested. It was shown that the HTC in the copper HX was much better than in the case of steel structures and approximately 18–25 times higher than in the case of polymer heat exchangers.

The current state of knowledge confirms the validity of researching this topic. The literature review contains significant gaps in the study of flow resistance in 3D-printed heat exchangers. The results of this experimental research will be used to determine the relationships describing flow resistance in structures based on triply periodic minimal surfaces, and it also enables us to specify the energy consumption of these devices and

compare the profitability of their use to conventional designs, i.e., shell-and-tube or plate heat exchangers.

2. Materials and Methods

Flow tests were carried out at the measuring station in the scope of the following parameters: 20 < Re < 200; mass flux: 4–24 kg/h; the of the working media temperature t_h, t_c was 50 °C, 20 °C, respectively.

The overall view of the test facility has been presented in Figure 1. The major element of the test stand is the 3D-printed gyroid-structured heat exchanger (1). Table 1 presents the measuring apparatus used in detail, the measuring range and the uncertainty level.

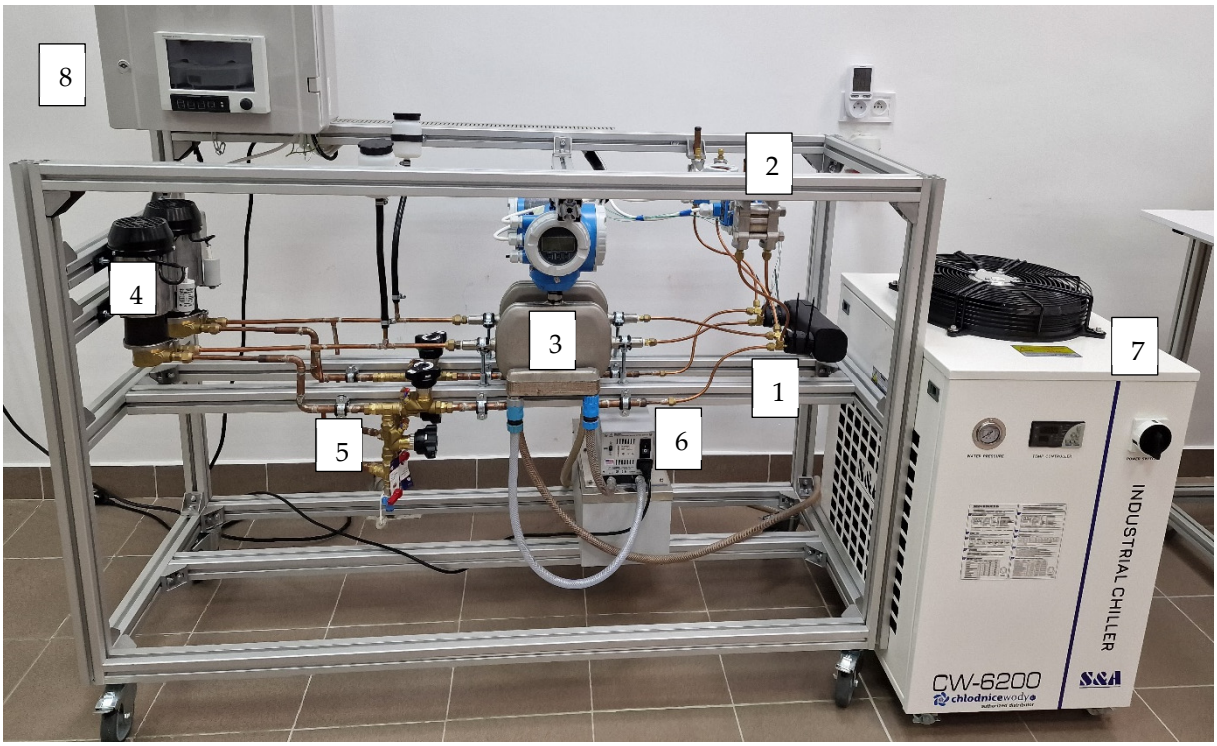

Figure 1. The overall view of the test facility: 1—the heat exchanger; 2—pressure drop sensors; 3—mass flow meters; 4—pumps; 5—regulating valves; 6—ultra thermostat; 7—chiller; 8—data acquisition unit.

Table 1. The measuring equipment's uncertainty level.

Value	Equipment	Range	Uncertainty
Mass flux ($\dot{m}$)	Coriolis flow meters	0–250 kg·h^{-1}	±0.1%
Pressure (p)	Pressure sensor	0–50 kPa	±0.05%
	Delta bar sensors	0–30 kPa	±0.075%
Temperature (T)	Thermometers	−40–+475 °C	±0.2 K

The uncertainty level is as given p = ±0.05% (max 100 kPa), Q = ±2% (max 5 W), T = ±0.2 K.

Figure 2 shows the overall view of the heat exchanger and the internal gyroid structure. Heat exchange took place between hot and cold fluid (water). Distilled and deionized water was used as the working fluid. The hot fluid, heated to the set temperature in an additional intermediate plate heat exchanger, was directed to the measuring section. The working fluid was heated indirectly using an ultra thermostat (6).

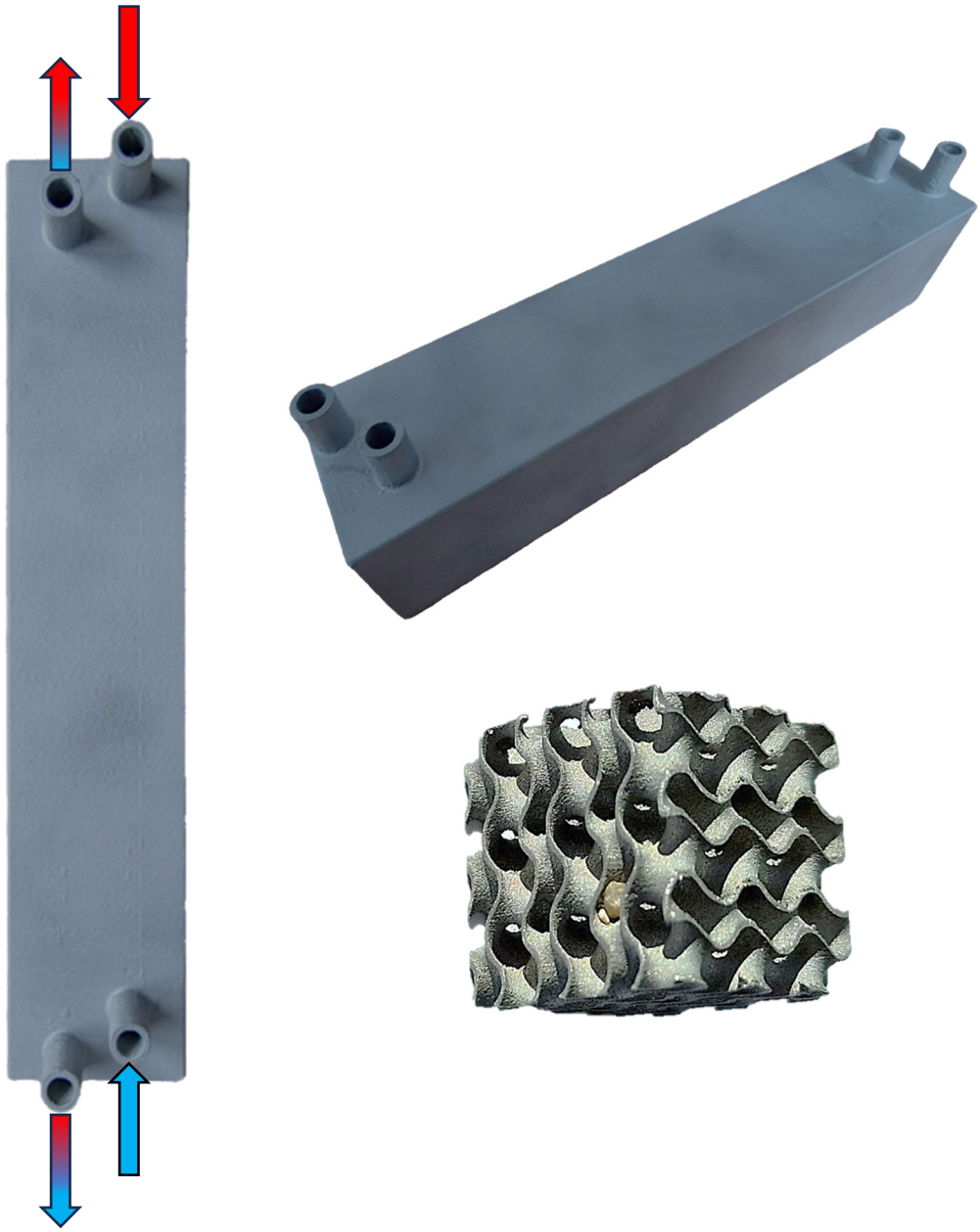

Figure 2. The view of the 3D-printed gyroid heat exchanger.

An additional cooling device (7) determined the temperature of the second working medium, the coolant. Magnetic pumps (4) forced the flow of both working media through the measuring section (Figure 3).

Precise control valves ensured a constant mass flow rate of the working media. Two differential manometers were installed on the measuring section to measure the pressure drop (8). The working fluids flowed through the heat exchanger (red/hot; blue/cold) in countercurrent.

The gyroid HX dimensions were 199.5 × 40.5 × 41.51 mm. The inner and outer diameters of the HX connections were di/de = 6/9 mm, respectively. The HX's lattice wall thickness was δ = 0.5 mm.

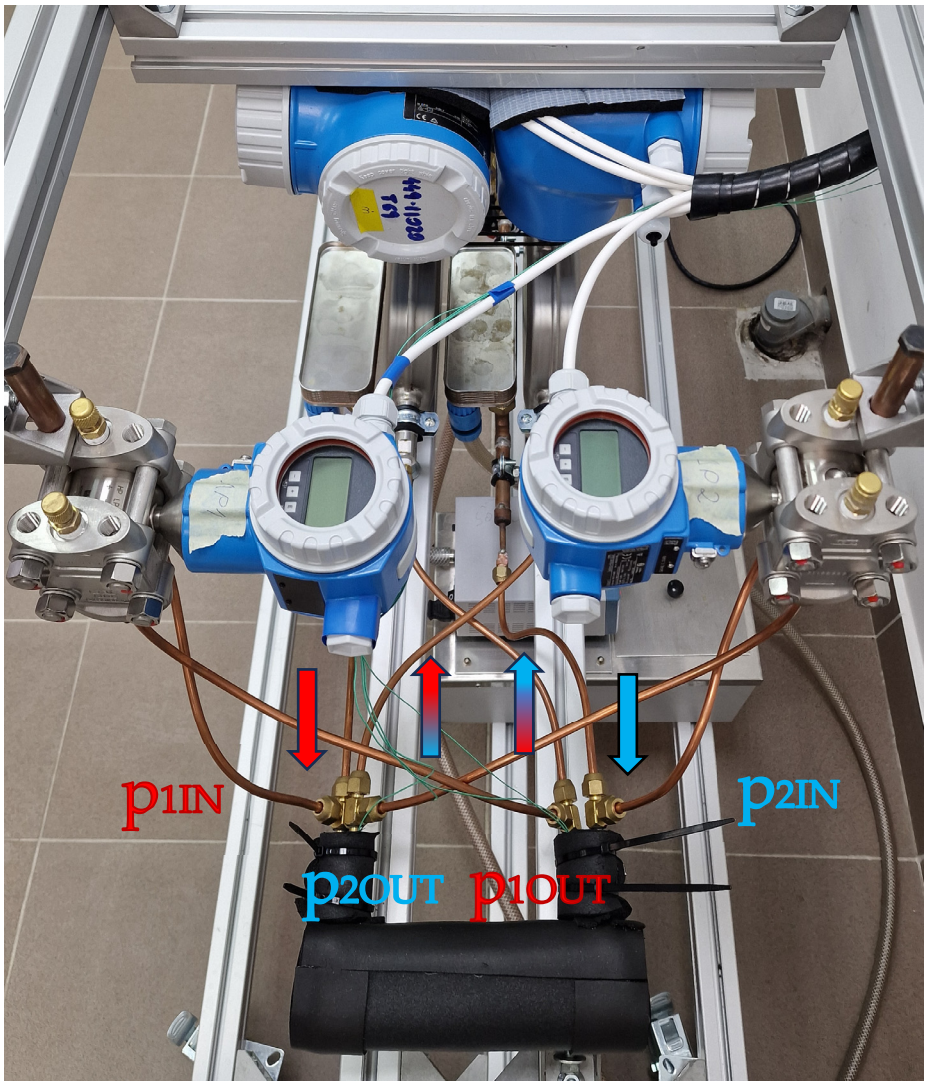

Figure 3. The measuring section.

3. Results and Discussion

The pressure drops of the single-phase flow of the base working fluids (water) are presented below. The Reynolds number was calculated according to Equation (1):

$$Re = \frac{wD_h}{\nu}, \tag{1}$$

where w [m/s] is the fluid velocity during TPMS channel flow, D_h [m] is the hydraulic diameter, and ν [kg/(ms)] is the kinematic viscosity coefficient.

The hydraulic diameter D_h was calculated according to Equation (2):

$$D_h = \frac{4V}{A_w}, \tag{2}$$

where V [m^3] is the heat exchanger volume, and A_w [m^2] is the TPMS wetted surface area.

The relationship between the pressure drop along the exchanger's length and the working fluid's mass flow rate is shown below in Figure 4.

As can be seen, the flow resistance increases with the mass flow rate. Similar behavior was noted during the flow of both fluids. The pressure drop values during hot fluid flow are slightly lower than cold fluid flow.

Figure 5 shows the dependency of the pressure drop on the Reynolds number. The pressure drop increases as the Reynolds number increases. The highest pressure drop values were noted for cold fluid flow at Reynolds number 140 < Re < 150. Lower pressure drop values were noted at the same Reynolds number values for the hot fluid. The friction factor f [-] was calculated based on the measurement data for pressure drop $\Delta p/l$ using the following formula:

$$f = \frac{\Delta p}{l} \frac{2D_h}{\rho w^2}, \tag{3}$$

where l [m] is the HX length, and ρ [kg/m^3] is the working fluid density.

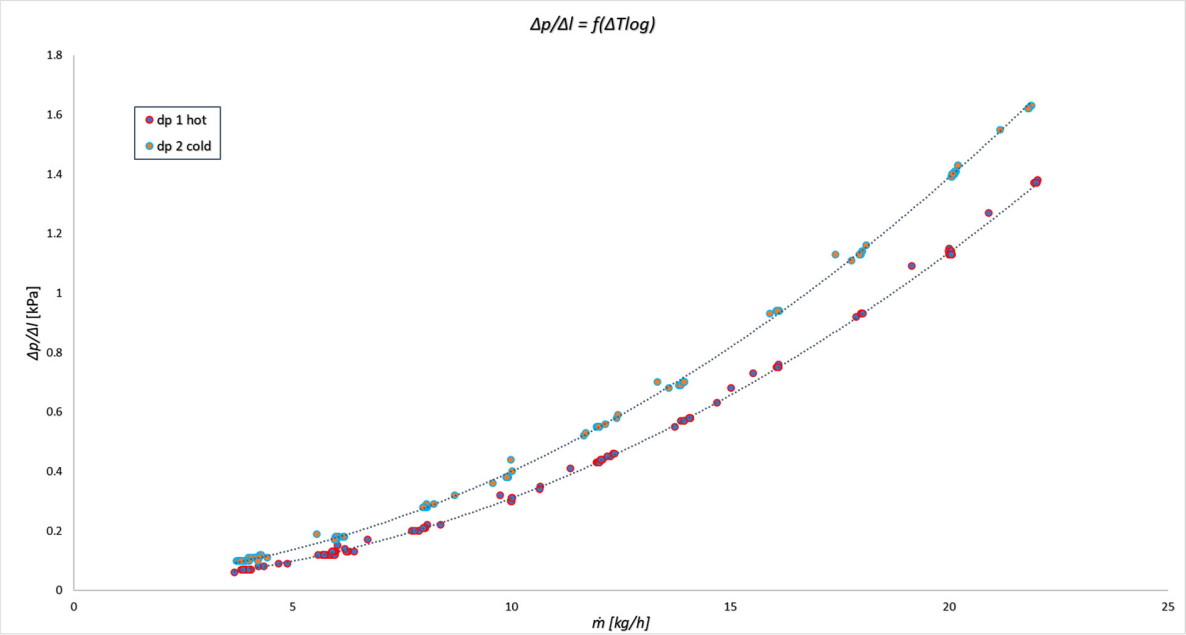

Figure 4. The dependence of local pressure drop on mass flow rate.

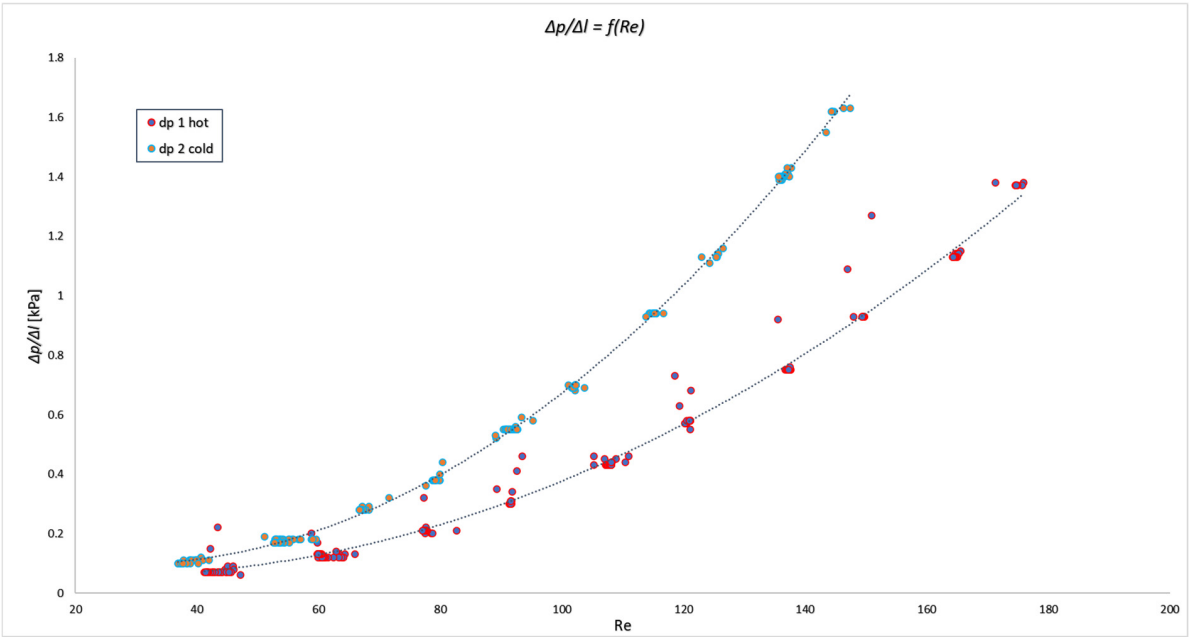

Figure 5. The dependence of local pressure drop on Reynolds number.

Figure 6 compares the experimental and simulation data [22–24] for the dependency between the experimental friction factor calculated using Equation (3) and the Reynolds number.

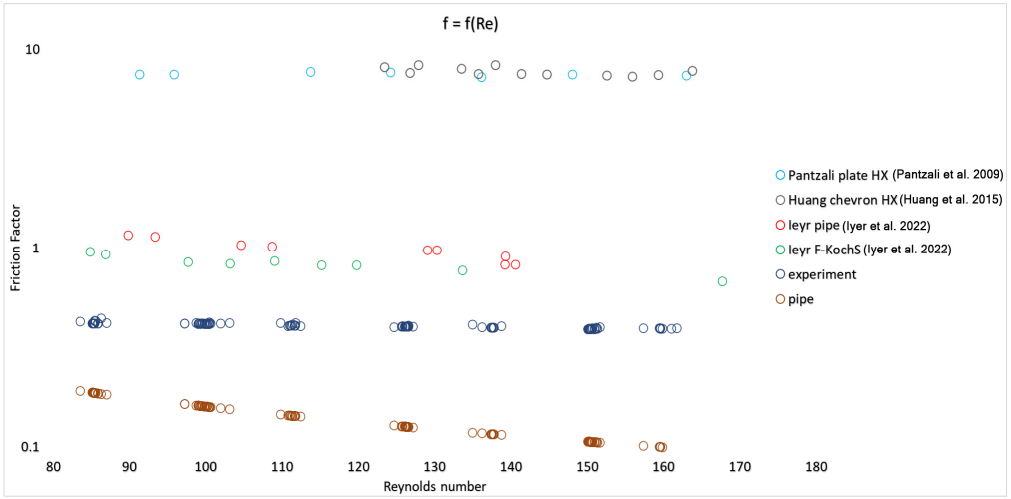

Figure 6. The dependency of local pressure drop on the mean logarithmic temperature difference [22–24].

The friction factor is calculated according to Equation (3) and is similar to that presented in the study [22]. Its values are slightly lower than those presented in the literature. Compared to a typical chevron heat exchanger design, the friction factor values presented by Huang et al. [23] are an average order of magnitude lower than for a gyroid heat exchanger of similar dimensions. For a change, the friction factor values calculated for a straight section of a circular cross-section according to the formula $f = 64/Re$ are lower than for the experiment.

Accordingly, a new relationship describing the friction factor in heat exchangers filled with a gyroidal structure was determined based on dimensional analysis. The relationship takes the following form:

$$f = 0.59Re^{-0.58}, \quad (4)$$

After applying the above modifications of the slope coefficients, high compliance of the test data with the calculated data can be seen in Figure 7, according to Equation (4).

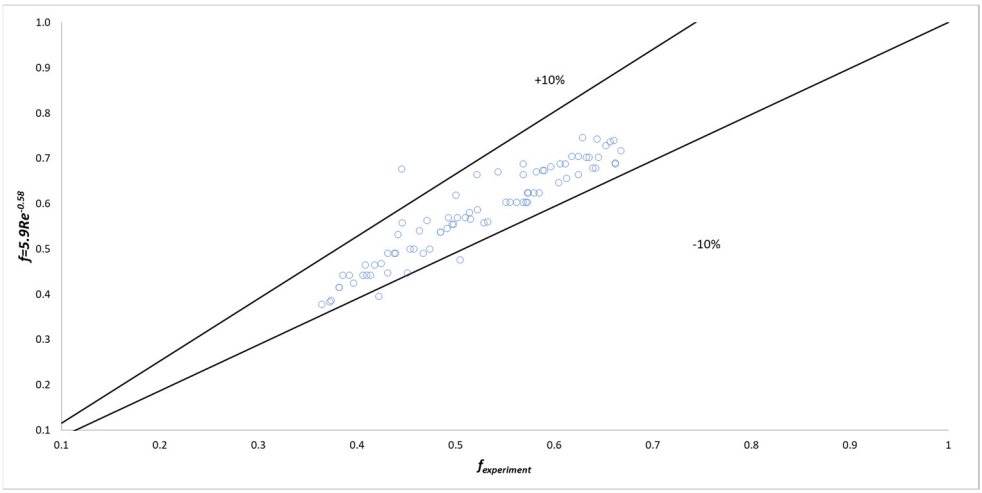

Figure 7. The dependency of the experimental friction factor with the values calculated according to Equation (4).

4. Conclusions

1. Experimental tests were carried out on a compact heat exchanger, a prototype designed and manufactured using the additive method from AISI 316L steel in 3D printing. The

device's design is based on a triple periodic minimum surface (TPMS) geometry, called a gyroid, which can only be achieved through additive manufacturing.
2. The study presents the results of flow tests determining pressure drops during the flow of working fluids under variable temperature and mass flow rate conditions.
3. The flow characteristics during the single-phase characteristics were determined, including $\Delta p/\Delta l = f(\dot{m})$. It was confirmed that in the case of a gyroidal geometry exchanger, the previously used classical relationships describing the flow resistance of working media do not apply.
4. Based on the test data of the pressure drop $\Delta p/l$, the values of the friction coefficient f were calculated for the flow of working media in the new type of heat exchanger. This enabled the development of the calculation relationship (4), which can be used to determine the value of f in heat exchangers filled with a gyroid structure.
5. The developed Equation (4) will be used to determine flow resistance in structures based on a TPMS. It will also enable us to determine the energy consumption of these devices and compare their profitability with conventional structures, i.e., tube-and-tube or plate heat exchangers.
6. Further studies are planned on flow resistance during heat transfer in 3D-printed heat exchangers and on the effectiveness of using mixtures of water and phase change materials as latent functional thermal fluids.

Author Contributions: Methodology, M.K.; Software, K.D.; Validation, T.B.; Investigation, K.D. and T.B.; Resources, M.K.; Data curation, M.K.; Writing—review and editing, M.K. All authors have read and agreed to the published version of the manuscript.

Funding: This research received no external funding.

Data Availability Statement: The original contributions presented in this study are included in the article. Further inquiries can be directed to the corresponding author.

Conflicts of Interest: The authors declare no conflicts of interest.

Nomenclature

Symbols	
A	tube cross-sectional area [m^2]
D_h	internal diameter of the tube [m]
l	tube length [m]
f	friction factor [-]
$\dot{m}$	mass flow rate [kg/s]
p	pressure [Pa]
w	average flow velocity[m/s]
Greek symbols	
ε	efficiency [-]
R	density [kg/m^3]
ν	kinematic viscosity coefficient [m^2/s]
μ	dynamic viscosity coefficient [Pa·s]
Abbreviations	
Re	Reynolds number [-]
cold	cold working fluid
F-KS	Fischer–Koch's structure
HX	heat exchanger
hot	hot working fluid
I-WP	Alan Schoen's Structure
TPMS	triply periodic minimal surface

References

1. Reynolds, B.W.; Fee, C.J.; Morison, K.R.; Holland, D.J. Characterisation of Heat Transfer within 3D Printed TPMS Heat Exchangers. *Int. J. Heat Mass Transf.* **2023**, *212*, 124264. [CrossRef]
2. Samson, S.; Tran, P.; Marzocca, P. Design and modelling of porous gyroid heatsinks: Influences of cell size, porosity and material variation. *Appl. Therm. Eng.* **2023**, *235*, 121296. [CrossRef]
3. Oh, S.H.; An, C.H.; Seo, B.; Kim, J.; Park, C.Y.; Park, K. Functional morphology change of TPMS structures for design and additive manufacturing of compact heat exchangers. *Addit. Manuf.* **2023**, *76*, 103778. [CrossRef]
4. Wang, J.; Chen, K.; Zeng, M.; Ma, T.; Wang, Q.; Cheng, Z. Investigation on flow and heat transfer in various channels based on triply periodic minimal surfaces (TPMS). *Energy Convers. Manag.* **2023**, *283*, 116955. [CrossRef]
5. Bonner-Hutton, O.; Busch, B.; Lv, Y.; Caughley, A.; Badcock, R.; Lumsden, G.; Weijers, H.; Singamneni, S. Analysis of gyroid heat exchangers for superconducting electric motors. *Mater. Today Proc.* **2023**. [CrossRef]
6. Tang, W.; Zhou, H.; Zeng, Y.; Yan, M.; Jiang, C.; Yang, P.; Li, Q.; Li, Z.; Fu, J.; Huang, Y.; et al. Analysis on the convective heat transfer process and performance evaluation of Triply Periodic Minimal Surface (TPMS) based on Diamond, Gyroid and Iwp. *Int. J. Heat Mass Transf.* **2023**, *201*, 123642. [CrossRef]
7. Tang, W.; Zou, C.; Zhou, H.; Zhang, L.; Zeng, Y.; Sun, L.; Zhao, Y.; Yan, M.; Fu, J.; Hu, J.; et al. A novel convective heat transfer enhancement method based on precise control of Gyroid-type TPMS lattice structure. *Appl. Therm. Eng.* **2023**, *230*, 120797. [CrossRef]
8. Brambati, G.; Guilizzoni, M.; Foletti, S. Convective heat transfer correlations for Triply Periodic Minimal Surfaces based heat exchangers. *Appl. Therm. Eng.* **2024**, *242*, 122492. [CrossRef]
9. Dassi, L.; Chatterton, S.; Parenti, P.; Vania, A.; Colosimo, B.M.; Pennacchi, P. Cooled pads with bioinspired gyroid lattice for tilting pad journal bearings: Experimental validation of numerical model for heat transfer. *Tribol. Int.* **2023**, *184*, 108448. [CrossRef]
10. Chen, F.; Jiang, X.; Lu, C.; Wang, Y.; Wen, P.; Shen, Q. Heat transfer efficiency enhancement of gyroid heat exchanger based on multidimensional gradient structure design. *Int. Commun. Heat Mass Transf.* **2023**, *149*, 107127. [CrossRef]
11. Dixit, T.; Al-Hajri, E.; Paul, M.C.; Nithiarasu, P.; Kumar, S. High performance, microarchitected, compact heat exchanger enabled by 3D printing. *Appl. Therm. Eng.* **2022**, *210*, 118339. [CrossRef]
12. Pelegatti, M.; Scalzo, F.; Sordetti, F.; Vaglio, E.; Magnan, M.; Totis, G.; Sortino, M.; Benasciutti, D.; Lanzutti, A.; De Bona, F.; et al. Low cycle fatigue behaviour of cellular materials: Experimental comparative study of strut-based and gyroid structures made of additively manufactured 316L steel. *Int. J. Fatigue* **2024**, *178*, 108024. [CrossRef]
13. Ramos, H.; Santiago, R.; Soe, S.; Theobald, P.; Alves, M. Response of gyroid lattice structures to impact loads. *Int. J. Impact Eng.* **2022**, *164*, 104202. [CrossRef]
14. Luo, J.W.; Chen, L.; Min, T.; Shan, F.; Kang, Q.; Tao, W.Q. Macroscopic transport properties of Gyroid structures based on pore-scale studies: Permeability, diffusivity and thermal conductivity. *Int. J. Heat Mass Transf.* **2020**, *146*, 118837. [CrossRef]
15. Moradmand, M.M.; Sohankar, A. Numerical and experimental investigations on the thermal-hydraulic performance of heat exchangers with Schwarz-P and gyroid structures. *Int. J. Therm. Sci.* **2024**, *197*, 108748. [CrossRef]
16. Yan, K.; Wang, J.; Li, L.; Deng, H. Numerical investigation into thermo-hydraulic characteristics and mixing performance of triply periodic minimal surface-structured heat exchangers. *Appl. Therm. Eng.* **2023**, *230*, 120748. [CrossRef]
17. Yan, K.; Deng, H.; Xiao, Y.; Wang, J.; Luo, Y. Thermo-hydraulic performance evaluation through experiment and simulation of additive manufactured Gyroid-structured heat exchanger. *Appl. Therm. Eng.* **2024**, *241*, 122402. [CrossRef]
18. Liang, D.; Yang, K.; Gu, H.; Chen, W.; Chyu, M.K. The effect of unit size on the flow and heat transfer performance of the "Schwartz-D" heat exchanger. *Int. J. Heat Mass Transf.* **2023**, *214*, 124367. [CrossRef]
19. Yan, G.; Sun, M.; Zhang, Z.; Liang, Y.; Jiang, N.; Pang, X.; Song, Y.; Liu, Y.; Zhao, J. Experimental study on flow and heat transfer performance of triply periodic minimal surface structures and their hybrid form as disturbance structure. *Int. Commun. Heat Mass Transf.* **2023**, *147*, 106942. [CrossRef]
20. Alteneiji, M.; Ali, M.I.H.; Khan, K.A.; Al-Rub, R.K.A. Heat transfer effectiveness characteristics maps for additively manufactured TPMS compact heat exchangers. *Energy Storage Sav.* **2022**, *1*, 153–161. [CrossRef]
21. Gao, S.; Ding, J.; Qu, S.; Liu, H.; Song, X. Numerical and experimental investigation of additively manufactured shell-lattice copper heat exchanger. *Int. Commun. Heat Mass Transf.* **2023**, *147*, 106976. [CrossRef]
22. Iyer, J.; Moore, T.; Nguyen, D.; Roy, P.; Stolaroff, J. Heat transfer and pressure drop characteristics of heat exchangers based on triply periodic minimal and periodic nodal surfaces. *Appl. Therm. Eng.* **2022**, *209*, 118192. [CrossRef]

23. Huang, D.; Zan, W.; Sunden, B. Pressure drop and convective heat transfer of Al_2O_3/water and MWCNT/water nanofluids in a chevron plate heat exchanger. *Int. J. Heat Mass Transf.* **2015**, *89*, 620–626. [CrossRef]
24. Pantzali, M.N.; Mouza, A.A.; Paras, S.V. Investigating the efficacy of nanofluids as coolants in plate heat exchangers (PHE). *Chem. Eng. Sci.* **2009**, *64*, 3290–3300. [CrossRef]